Identification of secondary fatty alcohols in atmospheric aerosols in temperate forests

Yuzo Miyazaki[1], Divyavani Gowda[1,2], Eri Tachibana[1], Yoshiyuki Takahashi[3], Tsutom Hiura[4]

[1]Institute of Low Temperature Science, Hokkaido University, Sapporo, 060-0819, Japan
5 [2]Now at RIKEN Center for Integrative Medical Science, Yokohama, 230-0045, Japan
[3]National Institute for Environmental Studies, Tsukuba, 305-8506, Japan
[4]Field Science Center for Northern Biosphere, Hokkaido University, Tomakomai, 053-0035, Japan

Correspondence to: Yuzo Miyazaki (yuzom@lowtem.hokudai.ac.jp)

10 **Abstract.** Fatty alcohols (FAs) are major components of surface lipids (waxes) and can act as surface-active organic aerosols in the atmosphere, influencing chemical reactions, particle lifetimes, and the formation of cloud droplets and ice nuclei. However, studies on the composition and source of the FAs in atmospheric aerosols are very limited. In this study, we identified five secondary FAs (SFAs) with C_{27} and C_{29} from aerosol samples collected throughout one year at two different deciduous forest sites in Japan. Fatty diols, such as *n*-heptacosan-5,10-diol, were identified in atmospheric aerosols for the first time.
15 Among the identified SFAs, *n*-nonacosan-10-ol was the most abundant compound, followed by *n*-nonacosan-5-10-diol at both of the forest sites. Concentrations of the SFAs exhibited distinct seasonal variation, with pronounced peaks during the growing season at each forest site. The SFAs showed significant correlation with sucrose, which is used as a molecular tracer of pollen. A significant fraction of the SFAs was attributed to the submicrometer particles in the growing season. The results indicate that they originated mostly from plant wax and could be used as useful tracers for primary biological aerosol particles.

1 Introduction

20 Lipids can be effectively used as molecular markers of terrestrial and marine sources of atmospheric aerosols (e.g., Gagosian et al, 1981). In the terrestrial environment, different organisms contain a variety of long-chain alcohols (fatty alcohols; FAs) because of the diversity of pathways used by the biota for the synthesis of molecules and other compounds. Most fatty alcohols occur in biota as waxes covering parts of plants, useful for preventing desiccation, protection from bacterial

25 attack, UV screening, and so on (e.g., Dahl et al., 2005). Because the main function of plant waxes is to reduce water loss through evaporation, waxes originating from this source tend to have longer chain lengths. The most prominent chain lengths are C_{26} to C_{30} (Tulloch, 1976). Once emitted into the atmosphere, FAs in atmospheric aerosols can act as tracers of primary biological aerosol particles (PBAPs) (Simoneit et al., 2004).

Because of their chemical structure and the similarity of parts of this structure to water, lipids are surface active. FAs are
30 known as major components of surface lipids (waxes) with chains varying between C_{20} and C_{34} carbon atoms (Mudge, 2005). Fatty alcohols are composed of long-chained hydrocarbons and hydroxyl (–OH) groups, which can congregate at the aqueous surface and can act as surface-active organic aerosols (OAs). These aerosols can cause gases to transfer into the aqueous phase as atmospheric particles and prevent evaporation, which influences chemical reactions, particle lifetimes, fog/cloud droplets, and ice nuclei (IN) (Gill et al. 1983; Cantrell and Robinson, 2006; Knopf et al., 2018). In particular, biogenic particles such as
35 fungal spores and bacteria can serve as a source of IN macromolecules, implying that IN macromolecules are therefore derived from a variety of biological or biogenic particles (Pummer et al., 2015). Long-chained alcohols show appreciable IN activity if they are crystallized into well-defined mono-layers. This depends on chain length, the position of the OH group, and any substitutions on the side chains (Popovitz-Biro et al., 1994).

Oros and Simoneit (2001a) observed *n*-nonacosan-10-ol, one of the secondary FAs (SFAs), in smoke samples from conifers subjected to controlled burning. In addition, an alkanediol *n*-nonacosan-5-10-diol was identified in ambient aerosol samples collected in the western North Pacific during the ACE-Asia campaign (Simoneit et, al., 2004). Some common alkanols were also found within ambient aerosols at urban and remote island sites, and are thought to have been emitted to the atmosphere

5   via biomass burning (Oros and Simoneit, 2001a, 2001b). These studies also indicate an input of waxes from forests consisting of both soft and hardwoods. However, studies are very limited on the composition and sources of FAs in atmospheric aerosols obtained in the vicinity of source regions, such as forest environments.

In this study, we used a gas chromatography (GC)-mass spectrometer (MS) to identify five SFAs found in atmospheric aerosols, both in submicrometer particles and the total suspended particulate matter (TSP), sampled throughout one year within

10   canopies of two different temperate forests in Japan. We discuss their possible sources based on their seasonal variations in mass concentration found at the two forest sites.

2 Experimental

2.1 Aerosol Sampling

15   Ambient aerosol samplings were conducted at two different forest sites in Japan (**Fig. 1**): One is the Tomakomai (TMK) Experimental Forest (42°43' N, 141°36' E) of Hokkaido University, located in northern Japan, and the other is the Fuji-Hokuroku (FHK) Flux Research site (35°26' N, 138°45' E). All the aerosol samples were collected on quartz fiber filters (25 cm × 20 cm), which were pre-combusted at 410°C for 6 hours to remove any contaminants. Descriptions of each site are given in the following subsections.

2.1.1 Tomakomai (TMK) Experimental Forest

The TMK site is situated in a cool-temperate zone, with its southern boundary adjacent to Tomakomai City and its industrial port area facing the Pacific Ocean. The mixed cool temperate forest consists of mature and secondary deciduous forest and manmade coniferous forest with various types of forest floor cover (Hiura 2001, 2005). The soil consists of shallow and unweathered volcanogenic regosols. The predominant local wind direction in autumn and winter is from the north, originating

25   in the forested areas. In contrast, air transported from the south (the coastal urban area) is dominant in summer.

At the TMK site, both TSP and submicrometer aerosol samples were collected continuously in parallel using two high-volume air samplers (HVASs; Model 120SL, Kimoto Electric, Osaka, Japan) at an altitude of ~18 m above the forest floor of the research site (Müller et al, 2017). A cascade impactor (CI; Model TE-234, Tisch Environmental, Cleves, OH, USA) was attached to one of the two HVASs to collect size-segregated particles with five stages at a flow rate of 1130 L min^{-1}. We used

30   analytical results obtained from the bottom stage of the impactor, which collected particles with aerodynamic diameter smaller than 0.95 μm. Aerosol particles within this size range are referred to as submicrometer particles. The sampling was taken continuously with a duration of approximately 1 week for each sample, from January to December in 2015. Collected filter samples were individually stored in glass jars with a Teflon-lined screwed cap at −20°C to limit the chance for chemical reactions on the filter and the loss of volatile compounds. In total, 23 sample sets were obtained at this site for both TSPs and

35   submicrometer particles.

2.1.2 Fuji-Hokuroku (FHK) Flux Research site

The FHK research site is located at the base of Mt. Fuji in Fujiyoshida City, Yamanashi, Japan (**Fig. 1**) (e.g., Mochizuki et al., 2015). The urban area of Fujiyoshida City is located about 8 km northeast of the site. The vegetation type is *Larix*

kaemperi plantation, which was planted uniformly 55 years ago over 150 ha. Tree height is approximately 20–25 m. The site is surrounded by coniferous and broad-leaved mixed forests. A meteorological tower of 32-m height and a steel scaffold of 20-m height for tree surveys are situated at the center of the forest site. The soil type is coarse-grained volcanic ash. The forest floor is predominantly covered with *Dryopteris crassirhizoma*. Further details of the study site are given by Urakawa et al.
5 (2015).

TSP sampling was conducted at a height of 16 m, just beneath the larch canopy, using a HVAS (Model 120SL, Kimoto Electric, Osaka, Japan) mounted on the 20-m steel scaffold. The aerosol samples were collected from January 2015 to December in 2016 with a sampling duration for each aerosol sample of ~2 weeks. The flow rate of the TSP sampling was approximately ~600 L min^{-1}. In total, 15 and 17 samples were analysed, obtained at the FHK site for the year 2015 and 2016,
10 respectively. The collected filter samples were kept frozen at −20°C until analysis.

2.2 Analytical Procedure with Gas Chromatography (GC)-Mass Spectrometer (MS)

For the aerosol samples, a filter cut of 3.8 cm^2 was extracted with dichloromethane/methanol (2:1, v/v) and the –OH functional groups in the extracted samples were reacted with a mixture of 50 µl of *N,O*-bis-(trimethylsilyl) trifluoroacetamide (BSTFA), 1% trimethyl chloride, and 10 µl pyridine to form trimethylsilyl (TMS) ethers. The TMS derivatives were then
15 analyzed for the presence of the compounds listed above using a capillary GC (GC7890, Agilent) equipped with a fused silica capillary column (DB-5MS, Agilent Technologies, Santa Clara, CA, USA) and coupled to a MS (MSD5975C, Agilent) (Miyazaki et al., 2012; Müller et al., 2017). From the TMS derivatives, structures of each compound of FAs were elucidated with electron ionization (EI) GC-MS, together with a GC-Time-of-Flight (TOF)-MS (JMS-T100GCV, JEOL). Identification of each compound was made based on GC retention time, literature mass spectra, and the interpretation of mass spectrometric
20 fragmentation patterns. In addition to FAs, sucrose and levoglucosan were also measured by the same method as described above.

3 Identification of Secondary Fatty Alcohols in the Aerosol Samples

Fig. 2 presents an example of a GC-MS total ion chromatogram (TIC) of the TMS extract of the TSP sample collected at
25 the FHK site. In previous studies, sugar compounds have been identified with the same method of derivatization, such as arabitol, fructose, glucose, and sucrose (e.g., Miyazaki et al. 2012; Müller et al., 2017). In the present study, P1–P5 refer to peaks which were identified to be TMS-derivatives of SFAs with carbon numbers of 27 and 29, the peaks of which appear in the latter part of the TIC.

Fig. 3 shows an EI mass spectra of P1–P5 obtained for the TMS derivatives with their molecular structures. On the basis
30 of the detailed interpretation of the EI mass spectral data together with their comparison to literature data (Yamamoto et al., 2008) as well as the exact mass measurements by GC-TOF-MS, the derivatives were assigned to (a) *n*-heptacosan-10-ol-TMS (P1; C$_{27}$), (b) *n*-heptacosan-5,10-diol-diTMS (P2; C$_{27}$), (c) *n*-nonacosan-10-ol-TMS (P3; C$_{29}$), (d) *n*-nonacosan-10-13-diol-diTMS (P4; C$_{29}$), and (e) *n*-nonacosan-5-10-diol-diTMS (P5; C$_{29}$). The spectra of *n*-heptacosan-10-ol-TMS is characterized by the presence of ion peaks at m/z 73, 229, and 341 (**Fig. 3a**). Similarly, the mass spectra of *n*-nonacosan-10-ol-TMS showed
35 that ion peaks at m/z 73, 229, and 369 are significant (**Fig. 3c**). The presence of ion peaks at m/z 73 was found for all the P1–P5, because TMS derivatives of compounds having –OH typically form [Si(CH$_3$)$_3$]. Indeed, the exact mass measurements by GC-TOF-MS confirmed the estimated composition of each peak. For example, the composition of P3 with M−15 was identified as C$_{31}$H$_{65}$OSi, where its theoretical and experimental m/z are 481.4805 and 481.4826, respectively, with an error of 4 ppm.

The spectra of P2 (**Fig. 3b**), P4 (**Fig. 3d**), and P5 (**Fig. 3e**) were identified as the TMS derivatives of secondary fatty diols. The mass spectra of *n*-nonacosan-10,13-diol-diTMS (**Fig. 3d**) is characterized by intense signals at m/z = 73, 229, 269, 327, and 367, whereas the spectra of *n*-nonacosan-5-10-diol-diTMS shows ion peaks at m/z = 159, 317, 369, and 527 (**Fig. 3e**). Spectra with significant ion peaks at m/z 73, 159, 317, and 341 are produced by *n*-heptacosan-5,10-diol-diTMS (**Fig. 3b**),

5   which was newly identified and is partly similar to the characteristics of the P1 and P5 spectra.

4 Seasonal Changes in the Concentrations of the Secondary Fatty Alcohols in the Aerosols at the Two Forest Sites

Fig. 4 displays the seasonal variations of the identified SFAs in the TSP samples at the TMK and FHK sites in 2015. Here seasonal categories of spring, summer, autumn, and winter refer to the periods March–May, June–August, September–

10   November, and December–February, respectively. The average concentrations in each seasonal category are summarized in **Table 1**. Among the SFAs identified, *n*-nonacosan-10-ol is the most abundant compound, followed by *n*-nonacosan-5,10-diol at both sites. The SFAs exhibited distinct seasonal changes with the largest concentrations observed in the spring (growing season), both at the TMK (101.7 ± 100.9 ng m^{-3}) and the FHK (211.7 ± 231.9 ng m^{-3}) sites. The maximum concentrations of *n*-nonacosan-10-ol reached 268.6 ng m^{-3} and 442.1 ng m^{-3} at the TMK and FHK sites, respectively. The SFA with the second

15   largest concentration, *n*-nonacosan-5,10-diol, showed a similar temporal variation to *n*-nonacosan-10-ol, suggesting that *n*-nonacosan-5,10-diol originated from identical or similar sources to those of *n*-nonacosan-10-ol. It is noted that the seasonal variation in concentrations of *n*-nonacosan-10-ol in 2016 was similar to that in 2015 at FHK (**Fig. 4b**). This similarity indicates that this seasonal trend is likely to be representative of the forest environment.

A primary plant origin of these SFAs is most likely, because the SFAs are known to be present in plant leaves; *n*-nonacosan-

20   10-ol has been identified as a major compound in epicuticular waxes found in gymnosperm species (Tulloch, 1976; Schulten et al., 1986), such as *Sequoiadendron giganteum* (Yamamoto et al., 2008). Moreover, secondary fatty diols have been reported in other plant species, such as *Pisum sativum* (Vioque and Kolattukudy, 1997). In the atmosphere, *n*-nonacosan-10-ol was observed in smoke aerosol samples from conifers subjected to controlled burning (Oros and Simoneit, 2001a). Moreover, some of the common alkanols found in urban and remote island sites are thought to have been emitted to the atmosphere by biomass

25   burning (Oros and Simoneit, 2001a, 2001b), while they also indicate an input of waxes from forests consisting of both soft and hardwoods.

In our study, a primary origin of biomass burning is unlikely because the SFAs showed no significant correlation with tracer compounds of biomass burning, such as levoglucosan with R^2 of <0.02 (data not shown) at both sites. Rather, the seasonal trends of the SFAs concentrations are similar to that of sucrose, which is an important primary saccharide of pollen

30   grains (Pacini, 2000) and has been used as a tracer for pollen (e.g., Miyazaki et al., 2012). Specifically, the concentration of *n*-nonacosan-10-ol showed significant positive correlations with that of sucrose both at the TMK ($R^2 = 0.70$) and FHK sites ($R^2 = 0.61$). The average concentrations of *n*-nonacosan-10-ol were significantly larger than those of sucrose in the growing season at the two sites. These results suggest that the increase in the mass concentrations of *n*-nonacosan-10-ol and the other SFAs is due to large emissions of wax from the forest leaves into the atmosphere. Our analysis also suggests that the SFAs identified

35   here can act as tracers for primary biological aerosol particles (PBAPs) which are surface active.

It is noted that the peak concentration of SFAs at FHK appeared in April (**Fig. 4b**), approximately one month earlier than at TMK (**Fig. 4a**). The difference in the appearance of the peaks is attributable to the difference in the growing season at the two sites: the growth of forest vegetation generally starts about one month earlier at FHK (35ºN) than at TMK (42ºN) (Nakaji et al., 2011; Takahashi et al., 2015), which is also evident from the seasonal changes in the net ecosystem production (Saigusa

40   et al., 2008). The primary emissions of these organic compounds clearly depend on the activity of the forest vegetation, and more specifically, plant leaf phenology at these forest sites. Considering that the aerosol sampling duration of about 1–2 weeks

is much longer than the time scale of transport of particles in the forest regions, the aerosol particles collected in this study were likely influenced by biogenic emissions from the whole area of each forest region.

Fig. 5 presents seasonal averages of the mass concentrations and particle size fractions of *n*-nonacosan-10-ol observed at the TMK site. The average values and their mass fractions to the TSP mass at TMK site in 2015 are also summarized in **Table**
5 **2**. In spring, the mass of *n*-nonacosan-10-ol in the submicrometer size ranges accounts for ~68% of the TSP mass, the fraction of which is much larger than that in summer (~10%) and autumn (~28%). Similarly, the average mass fraction of submicrometer *n*-nonacosan-5,10-diol in TSP is 65% in spring, whereas the mass fraction is 1% and 15% in summer and autumn, respectively. Our result is similar to that of Kavouras and Stephanou (2002), who also measured particle size distributions of *n*-alkanols (<C$_{26}$) at Eucalyptus and conifer forests in summer to show clear bimodal size distributions with
10 ~40% of the mass residing in particles with diameters smaller than 0.96 μm. In general, the majority of the mass of PBAPs reside in supermicrometer particles. Indeed, the mass fractions of sucrose in submicrometer size range were 29% in spring, showing the majority (~70%) of the mass resides in the supermicrometer size range in the growing season (**Table 2**). In contrast to the typical PBAPs tracers, our result suggests that a significant fraction of the SFAs can be attributed to the submicrometer particles in the growing season.

15

5 Conclusions

Secondary fatty alcohols with carbon numbers of 27 and 29 were identified in atmospheric aerosol samples collected throughout the year at two different deciduous forest sites. As far as we know, this study is the first to identify fatty diols, such as *n*-heptacosan-5,10-diol, in atmospheric aerosol samples and to show the seasonal variations in their concentrations in the
20 forest atmosphere.

Among the identified SFAs, *n*-nonacosan-10-ol was the most abundant molecular compound, followed by *n*-nonacosan-5,10-diol. The SFAs showed pronounced peaks in the growing season at both forest sites. In spring, the concentrations of *n*-nonacosan-5,10-diol were much larger than those of sucrose. Moreover, the concentrations of the identified SFAs showed significant positive correlations with those of sucrose at the two sites. These results indicate that the SFAs originated mostly
25 from plant wax. The difference in the peak appearance of the SFA concentrations at the two sites indicates that the primary emissions of these organic compounds clearly reflect the activity of the forest vegetation such as plant leaf phenology at the forest sites.

In the growing season, the fraction of *n*-nonacosan-10-ol in the submicrometer size range accounted for ~70% of the TSP mass. Similarly, the average mass of submicrometer *n*-nonacosan-5,10-diol in TSP accounted for 65% of the mass of TSP in
30 spring. These fractions were much larger than those in the other seasons, suggesting that a significant fraction of the SFAs was attributed to the submicrometer particles in the growing season. This study demonstrates that the SFAs identified, particularly *n*-nonacosan-10-ol and *n*-nonacosan-5,10-diol, can be used as effective tracers for PBAPs with surface-active organic matter.

Author contributions.

35 YM designed the research, led the overall study, and wrote the manuscript. DG performed the experiments with the GC-MS. TH and YT coordinated the aerosol samplings at the research sites. YT and YM made aerosol samplings. DG, YM, and ET analyzed the data.

Competing interests.

The authors declare that they have no conflict of interest.

Acknowledgements.

This research was supported by Grants-in-Aid for Scientific Research (B) (16H02931) from the Ministry of Education, Culture,
5   Sports, Science and Technology (MEXT), Japan. We thank the staff of Instrumental Analysis Division in Global Facility
Center of Creative Research Institution in Hokkaido University for their help with the GC-TOF-MS measurements of the
samples.

References

10   Cantrell, W., and Robinson, C.: Heterogeneous freezing of ammonium sulfate and sodium chloride solutions by
long chain alcohols, Geophys. Res. Lett., 33, L07802, doi:10.1029/2005GL024945, 2006.

Dahl, K. A., Oppo, D. W., Eglinton, T. I., Hughen, K. A., Curry, W. B., and Sirocko, F.: Terrigenous plant wax inputs to the
Arabian Sea: Implications for the reconstruction of winds associated with the Indian Monsoon, Geochimica et
Cosmochimica Acta 69(10), 2547–2558, 2005.

15   Gagosian R. B., Peltzer, E. T., and Zafiriou, O. C.: Atmospheric transport of continentally derived lipids to the tropical North
Pacific, Nature, 291, 312–314, 1981.

Gill, P. S., Graedel, T. E., and Weschler, C. J.: Organic films on atmospheric aerosol particles, fog droplets, cloud
droplets, rain-drops, and snowflakes, Rev. Geophys. Space Phys., 21, 903–920, 1983.

Hiura, T.: Stochasticity of species assemblage of canopy trees and understory plants in a temperate secondary forest created
20   by major disturbances, Ecological Research, 16, 887–893, 2001.

Hiura, T.: Estimation of aboveground biomass and net biomass increment in a cool temperate forest on a landscape scale,
Ecological Research, 20, 271–277, 2005.

Kavouras, I. G., and Stephanou, E.G.: Particle size distribution of organic primary and secondary aerosol in urban,
background marine, and forest atmosphere, J. Geophys. Res., 107(D8), 4069, doi:10.1029/2000JD000278, 2002.

25   Knopf, D. A., Alpert, P. A., and Wang, B.: The role of organic aerosol in atmospheric ice nucleation: A review, ACS Earth
Space Chem., 2 (3), 168–202, doi:10.1021/acsearthspacechem.7b00120, 2018.

Miyazaki, Y., Fu, P. Q., Kawamura, K., Mizoguchi, Y., and Yamanoi, K.: Seasonal variations of stable carbon isotopic
composition and biogenic tracer compounds of water-soluble organic aerosols in a deciduous forest, Atmos. Chem. Phys.,
12, 1367–1376, doi:10.5194/acp-12-1367-2012, 2012.

30   Mochizuki, T., Miyazaki, Y., Ono, K., Wada, R., Takahashi, Y., Saigusa, N., Kawamura, K., and Tani, A: Emissions of
biogenic volatile organic compounds and subsequent formation of secondary organic aerosols in a *Larix kaempferi* forest,
Atmos. Chem. Phys., 15, 12029–12041, doi:10.5194/acp-15-12029-2015, 2015.

Mudge, S. M.: Fatty alcohols–a review of their natural synthesis and environmental distribution. Exec Summ Soap Deterg
Assoc., 132, 1–141, 2015.

35   Müller, A., Miyazaki, Y., Tachibana, E., Kawamura, K., and Hiura, T.: Evidence of a reduction in cloud condensation nuclei
activity of water-soluble aerosols caused by biogenic emissions in a cool-temperate forest. Sci. Rep. 7, 8452,
doi:10.1038/s41598-017-08112-9, 2017.

Nakaji, T., Oguma, H. and Hiura, T.: Ground-based monitoring of the leaf phenology of deciduous broad-leaved trees using
high resolution NDVI camera images. J. Agri. Met., 67, 65-74, 2011.

Oros, D. R. and Simoneit, B. R. T.: Identification and emission factors of molecular tracers in organic aerosols from biomass burning Part 1. Temperate climate conifers. Appl. Geochem., 16, 1513–1544, 2001a.

Oros, D. R. and Simoneit, B. R. T.: Identification and emission factors of molecular tracers in organic aerosols from biomass burning Part 2. Deciduous trees. Appl. Geochem., 16, 1545–1565, 2001b.

5   Pacini, E.: From anther and pollen ripening to pollen presentation, Plant Syst. Evol., 222, 19-43, 2000.

Popovitz-Biro, R., Wang, J. L., Majewski, J., Shavit, E., Leis-erowitz, L., and Lahav, M.: Induced freezing of supercooled water into ice by self-assembled crystalline monolayers of am-phiphilic alcohols at the air-water interface, J. Am. Chem. Soc., 116, 1179–1191, 1994.

Pummer, B. G., Budke, C., Augustin-Bauditz, S., Niedermeier, D., Felgitsch, L., Kampf, C. J., Huber, R. G., Liedl, K. R.,

10   Loerting, T., Moschen, T., Schauperl, M., Tollinger, M., Morris, C. E., Wex, H., Grothe, H., Pöschl, U., Koop, T.; Fröhlich-Nowoisky, J.: Ice nucleation by water-soluble macromolecules, Atmos. Chem. Phys., 15 (8), 4077−4091, 2015.

Saigusa N., Yamamoto S., Hirata R., Ohtani Y., Ide R., Asanuma J., Gamo M., Hirano T., Kondo H., Kosugi Y.: Temporal and spatial variations in the seasonal patterns of CO2 flux in boreal, temperate, and tropical forests in East Asia. Agric. For. Meteorol., 148, 700-713, 2008.

15   Schulten, H.-R., Simmleit, N., and Rump, H. H.: Soft ionization mass spectrometry of epicuticular waxes isolated from coniferous needles, Chem. Phys. Lipids, 41, 209-224, 1986.

Simoneit, B. R. T., Kobayashi, M., Mochida, M., Kawamura, K., Lee, M., Lim, H.-J., Turpin, B. J., and Komazaki, Y.: Composition and major sources of organic compounds of aerosol particulate matter sampled during the ACE-Asia campaign. J. Geophys. Res., 109, D19S10, doi:10.1029/2004JD004598, 2004.

20   Takahashi Y., Saigusa N., Hirata R., Ide R., Fujinuma Y., Okano T., Arase T.: Characteristics of temporal variations in ecosystem CO_2 exchange in a temperate deciduous needle-leaf forest in the foothills of a high mountain. J. Agri. Met., 71, 4, 302-317, 2015.

Tulloch, A. P.: Chemistry of waxes of higher plants, chemistry and biochemistry of natural waxes. P. E. Kolattukudy. Amsterdam, Elsevier, 235–287, 1976.

25   Urakawa, R., Ohte, N., Shibata, H., Tateno, R., Hishi, T., Fukushima, K., Inagaki, Y., Hirai, K., Oda, T., Oyanagi, N., Nakata, M., Toda, H., Tanaka, K., Fukuzawa, K., Watanabe, T., Tokuchi, N., Nakaji, T., Saigusa, N., Yamao, Y., Nakanishi, A., Enoki, T., Ugawa, S., Hayakawa, A., Kotani, A., Kuroiwa, M., and Isobe, K.: Biogeochemical nitrogen properties of forest soils in the Japanese archipelago, Ecol. Res., 30, 1-2, doi:10.1007/s11284-014-1212-8, 2015.

Vioque, J. and Kolattukudy, P. E.: Resolution and purification of an aldehydegenerating and an alcohol-generating fatty

30   acyl-CoA reductase from pea leaves (Pisum sativum L). Archives of Biochemistry and Biophysics, 340, 1, 64-72, 1997.

Yamamoto, S., Otto, A., and Simoneit, B. R. T.: GC-MS analysis of wax in leaf of *Sequoiadendron giganteum*, Sequoioideae, Cuprressaceae. (in Japanese) Res. Org. Geochem. 23/24, 159–171, 2008.

Table 1. The mass concentrations[a] of the secondary fatty alcohols (SFAs) identified and sucrose in TSP at TMK and FHK sites in each season in 2015.

	TMK 2015				FHK 2015			
	Winter	Spring	Summer	Autumn	Winter	Spring	Summer	Autumn
n-Heptacosan-10-ol	0.34±0.16	1.85±1.90	0.27±0.32	0.31±0.23	0.54±0.40	4.37±4.86	0.78±0.38	0.34±0.28
n-Heptacosan-5,10-diol	N.D.	0.68±0.64	0.13±0.12	0.04±0.06	0.22±0.25	1.93±2.22	0.25±0.23	0.10±0.12
n-Nonacosan-10-ol	24.1±11.1	101.7±100.9	13.3±12.3	23.5±13.9	68.5±40.8	211.7±231.9	28.9±19.1	22.8±15.2
n-Nonacosan-10,13-diol	0.37±0.16	2.12±2.23	0.24±0.28	0.42±0.32	1.40±0.79	4.47±4.79	0.67±0.30	0.51±0.44
n-Nonacosan-5,10-diol	0.80±0.38	8.36±8.76	0.99±1.03	1.34±0.78	2.59±1.96	18.7±21.1	2.35±1.50	1.72±1.54
Sucrose	0.33±0.10	21.5±12.9	3.51±0.67	0.69±0.29	0.14±0.10	23.2±14.4	0.12±0.08	0.16±0.03

[a]Values are averages (ng m^{-3}) with ±1 standard deviation.

Table 2. The average concentrations of *n*-Nonacosan-10-ol, *n*-Nonacosan-5,10-diol, and sucrose in the submicrometer particles and their mass fractions to the TSP mass at TMK site in 2015.

	n-Nonacosan-10-ol[a]	Sub-μm/TSP ratio of *n*-Nonacosan-10-ol[b]	*n*-Nonacosan-5,10-diol[a]	Sub-μm/TSP ratio of *n*-Nonacosan-5,10-diol[b]	Sucrose[a]	Sub-μm/TSP ratio of sucrose[b]
Spring	69.56±125.40	0.684±1.981	5.24±11.71	0.648±2.393	6.28±6.27	0.292±0.116
Summer	1.26±0.69	0.095±0.010	0.01±0.02	0.010±0.001	0.28±0.36	0.080±0.011
Autumn	6.66±6.80	0.284±0.112	0.20±0.39	0.149±0.092	0.25±0.18	0.362±0.191

[a]Values are average concentrations (ng m^{-3}) with ±1 standard deviation.
[b]Values are average ratios (ng ng^{-1}) with ±1 standard deviation.

Figure 1: Locations of the two forest sites where aerosol sampling was made.
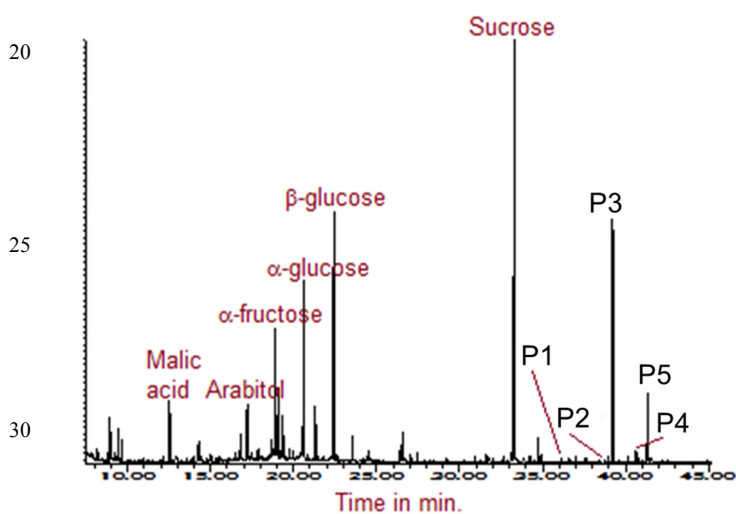
Figure 2: GC-MS total ion chromatogram obtained for the TMS derivatives. P1–P5 refer to peaks, which correspond to the secondary fatty alcohols identified in this study.

15

20

25

30
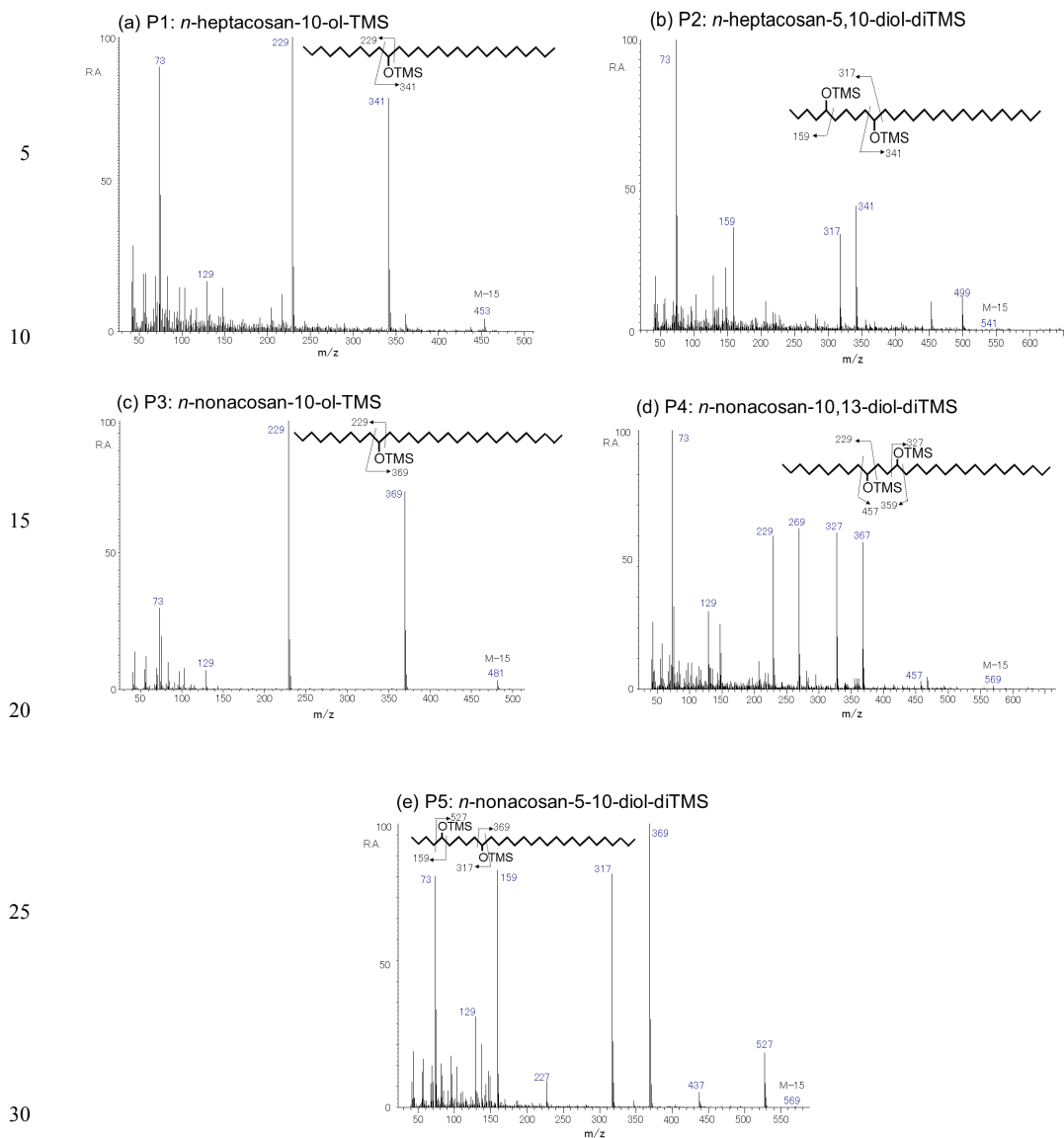
Figure 3: EI mass spectra obtained for the TMS derivatives of the identified secondary fatty alcohols. (a) P1: *n*-heptacosan-10-ol-TMS, (b) P2: *n*-heptacosan-5,10-diol-diTMS, (c) P3: *n*-nonacosan-10-ol-TMS, (d) P4: *n*-nonacosan-10,13-diol-diTMS, and (e) P5: *n*-nonacosan-5,10-diol-diTMS.

35

15
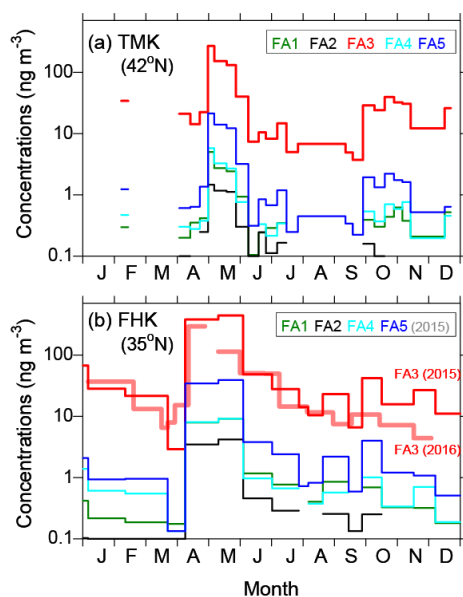
Figure 4: Temporal variations in the mass concentrations of the fatty alcohols (FAs) in the TSP samples at (a) TMK and (b) FHK
20 **sites in 2015. FA1: *n*-heptacosan-10-ol, FA2: *n*-heptacosan-5,10-diol, FA3: *n*-nonacosan-10-ol, FA4: *n*-nonacosan-10,13-diol, and FA5: *n*-nonacosan-5-10-diol. The data of FA3 in 2016 is also shown for comparison.**

25

30

35
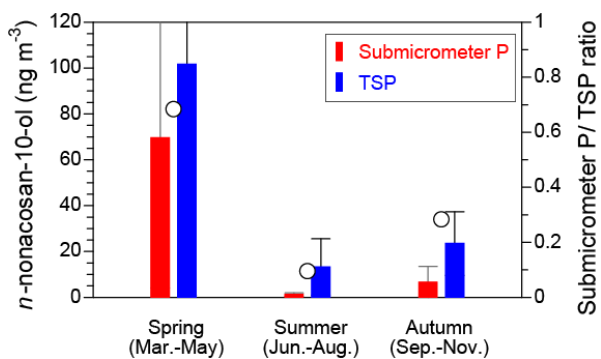
Figure 5: Seasonal averages of the mass concentrations of *n*-nonacosan-10-ol in the submicrometer particles (P) (red) and TSP (blue) samples obtained at the TMK site. The error bars show the standard deviations, and open circles indicate the mass ratios of the P/TSP.

40